Available online at www.sciencedirect.com
SCIENCE DIRECT®
Journal of Nuclear Materials 347 (2005) 111–117
journal of nuclear materials
www.elsevier.com/locate/jnucmat

Incident energy dependence of blistering at tungsten irradiated by low energy high flux deuterium plasma beams

G.-N. Luo *, W.M. Shu, M. Nishi

Tritium Engineering Laboratory, Japan Atomic Energy Research Institute, Tokai-mura, Naka-gun, Ibaraki 319-1195, Japan

Received 29 November 2004; accepted 29 July 2005

Abstract

Polycrystalline tungsten samples have been irradiated at near room temperature by high flux (1×10^{22} D/m^2/s) deuterium plasma beams with incident ion energies ranging 7–98 eV/D. Surface blistering occurred at all energies as observed by means of scanning electron microscopy. At all energies, the blisters increased in their size and number with fluence within the corresponding low fluence ranges. The size increase tended to saturate at certain fluences within the experimental fluence ranges, which might be attributed to rupturing of blisters. The critical fluence for blistering Φ_{cr} was found to increase with decreasing the incident energy. At energies <20 eV/D, Φ_{cr} increased more rapidly. This energy dependence of Φ_{cr} may be explained by a proposed model dealing with the oxide barrier to deuterium uptake into and release from the bulk W. The presence of oxide layers of some monolayers on the surfaces was verified by means of X-ray photoelectron spectroscopy analysis and secondary ion mass spectroscopy before and after irradiation to different fluences.

PACS: 61.80.Jh; 61.82.Bg; 68.35.Bs

1. Introduction

A firm basis has been established for demonstration of the scientific and technological feasibility of controlled fusion through continuous efforts on magnetically confined fusion [1,2]. However, the choice of armor materials for the divertor and first wall is still a critical issue regarding a future reactor, including the International Thermonuclear Experimental Reactor (ITER), towards a long term steady state operation [3]. Tungsten and its alloys have been considered as candidate armor material for part of the ITER divertor and the whole first wall in the further DEMO reactors [4], due to their acceptable thermo-mechanical properties, possible advantage of very low or negligible erosion at low plasma temperatures, and a moderate uptake of tritium [5].

The ITER divertor may be operated in a scenario of semi-detached plasma condition in order to reduce particle and heat fluxes onto the divertor plate [1], and the incident particle energy will range from <1 eV till 100 eV, whereas the flux will be as high as 10^{22}/m^2/s on average. In the past, hydrogen–metal interactions were studied overwhelmingly in incident energy of keV or higher and flux of 10^{20}/m^2/s or lower by using ion beam accelerators, as reviewed by Myers et al. [6], and the radiation-induced defects in the bulk and at the surface played a key role in hydrogen reemission, retention, and permeation

* Corresponding author. Tel.: +81 29 282 6452; fax: +81 29 282 5917.
E-mail address: luo@tpl.tokai.jaeri.go.jp (G.-N. Luo).

0022-3115/$ - see front matter © 2005 Elsevier B.V. All rights reserved.
doi:10.1016/j.jnucmat.2005.07.014

processes. Recently, investigations of irradiation of hydrogen isotope ions on tungsten under energies around 100 eV have been carried out by using both ion accelerators and plasma generators [7–11], showing clearly blistering at the W surfaces irradiated at temperatures from room temperature to ~900 K although the incident energies were too low to generate directly radiation defects in the bulk. So far, the circumstances under which blistering at W is favored, and especially how it may evolve and affect hydrogen retention in W and component lifetime has not yet been understood well.

In this paper, blistering behavior has been investigated at W irradiated using a newly established plasma generator [12], in which a deuterium plasma beam was produced and delivered onto sample. The incident energy was controlled from 100 eV down to some eV. The energy dependence of blistering has been studied systematically at near room temperature for the first time within this very low energy range, which should be beneficial to fundamental understanding on the mechanisms of blistering at W, and further hydrogen retention in and permeation through W.

2. Experimental

Tungsten plates (A.L.M.T. Corp.) were prepared by powder-metallurgy and hot-rolled reduction, and then heat treated at 1473 K for 30 min for stress relief as the standard final step before storing or cold working like grinding and polishing. The plates were subsequently cut and double-sided polished into samples of $10 \times 10 \times 2$ mm before shipping to our laboratory. The tungsten material has a purity of 99.99 wt% and the principal impurities in weight ppm are Mo and Fe ~10, C and O < 30. The as-shipped samples were irradiated without any more pretreatment prior to loading into chamber, except cleaning in an acetone ultrasonic bath.

The linear plasma generator [12] used in this study is capable of delivering plasma beams comparable to the practical edge plasma at ITER divertor. The generator consists of sections of vacuum chamber and pumping, cooling water, gas admittance, power supply, plasma generation, plasma delivery, sample holder, and plasma diagnosis. The achievable background pressure is lower than 5×10^{-6} Pa. The water-cooled sample holder is isolated from the grounded chamber wall so that the sample can be negatively biased to adjust the energy of ions impinging onto the sample. A single Langmuir probe is equipped about 3 cm upstream from the sample to obtain basic plasma parameters. The ion species in the plasma beam can be controlled via adjusting various parameters and measured using a differentially pumped quadrupole mass spectrometer (QMS) system as described in [13]. The species in the plasma beam generated in this work were determined to be predominantly D_2^+. And a fixed flux of 5×10^{21} $D_2^+/m^2/s$ (equivalent to 1×10^{22} $D/m^2/s$) was used in the experiments. The incident energy was varied via changing the bias voltage applied to the sample. The following bias voltages were employed, −200/−140/−80/−50/−30 V, resulting in the incident energies of 98/68/38/23/13 eV/D, respectively, taking simultaneously into account the plasma potential of ~−4 V measured by the Langmuir probe. An even lower energy of 7 eV/D was achieved by floating the sample, resulting in a floating potential of ~−18 V. The incident fluence was controlled by varying the irradiation time. The working pressure within the chamber was kept at ~1 Pa (D_2). The cooling water to sample holder was turned on to its full capacity of 2.6 l/min at 0.5 MPa and the temperature before irradiation was always about 293 K. The temperature rise of the sample being irradiated did not exceed 6 K during any irradiations, monitored by a type K thermocouple tightly pressing the rear of the sample.

The irradiated samples were observed at a tilt angle of 45° with a scanning electron microscope (SEM) in our laboratory (JEOL, JSM5410) to examine the occurrence and evolution of surface blistering. The judgment of blister appearance was limited by the resolution of the SEM employed that is not easy to distinguish blisters smaller than ~0.1 μm. Another SEM (Keyence, VE-7800) was used to observe surfaces of some of the samples and the cross-section of a sample prepared by means of focused ion beam (FIB) milling for better understanding the structure of blisters. X-ray photoelectron spectroscopy (XPS) in our laboratory (PERKIN ELMER PHI 1600) was employed to analyze the sample surfaces unirradiated and irradiated, with AlKα as the X-ray source, exposure area of 2×2 mm^2, and detected area of 0.8 mm^2. Depth profiles of the surface layers were obtained by means of secondary ion mass spectroscopy (SIMS) (Φ Physical Electronics, PHI ADEPT 1010) with the following beam parameters, Cs^+ beam energy of 5 keV, beam current of 10 nA, beam size of ~30 μm, incident angle of 60° from the surface normal, raster area of 400×400 μm^2. Negative secondary ions were detected from the central part of the raster area through an electronic aperture of 100×100 μm^2. The sputtering rate was estimated to be ~0.015 nm/s by means of a surface profiler (Veeco Corp., Dektak^{3}ST) that measures the height of step created by the sputtering at the surface.

3. Results and discussion

3.1. Surface morphology with varying the incident energy and fluence

At each incident energy, blisters were found at the irradiated surface of W samples after a corresponding

critical fluence was achieved. Fig. 1 shows the surface morphology with varying the incident energy and fluence. Results of three energies of 98/38/7 eV/D are shown in the figure, with different fluence ranges. For the 98 eV/D irradiation, the fluence of 3×10^{23} D/m^2 results in scattered formation of relatively small and low blisters. With increasing the fluence to 3×10^{24} D/m^2, blisters increases in number and diameter. Further increasing the fluence to 3×10^{25} D/m^2 brings forth more blisters; however the maximum diameter does not increase significantly except that some rare big blisters of ~3 μm may form due to merging of closely neighboring blisters. This merging is depicted more clearly in the image of 7 eV/6×10^{25} D/m^2 irradiation, where the intermediate stage is shown for two or three blisters merging into one, as pointed out by the arrows. The 38 eV/D irradiation does not induce visible blistering at the fluence of 3×10^{23} D/m^2, blisters appear soon with raising the fluence, and then evolves the same as for the 98 eV/D case. In the case of 7 eV/D irradiation, the fluence as large as 3×10^{25} D/m^2 only produces two very small blisters in the image, as indicated by the arrows, and then again the blistering follows the same way as for the other two energies. Results for the energies other than those appeared in Fig. 1 also show the similar fluence tendency for blistering. Blistering at such low energies as applied in this study (some eV to some 10 eV) has not yet been reported before. Another finding is that the increase in blister size seemed to saturate at certain fluences dependent on the incident energies, as shown in Fig. 2, and the maximum diameter was about 2–3 μm within the experimental fluence ranges.

In general, hydrogen implanted into tungsten will either diffuse back to the surface where the hydrogen atoms recombine into molecules and then desorb from the surface, or diffuse deeper into the material. The

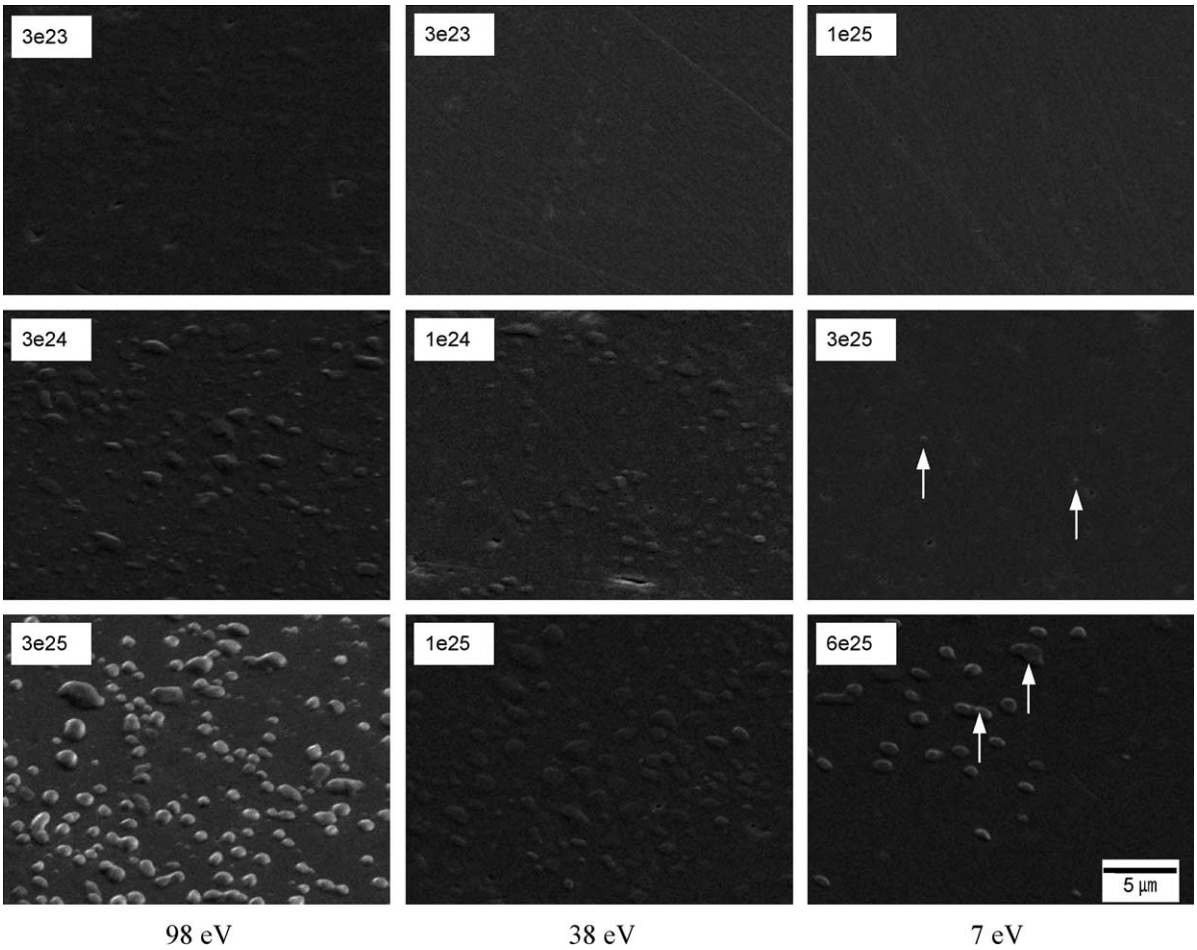

Fig. 1. Surface morphology of samples irradiated under three incident energies of 98, 38, and 7 eV, and different fluences as indicated in each image in D/m^2.

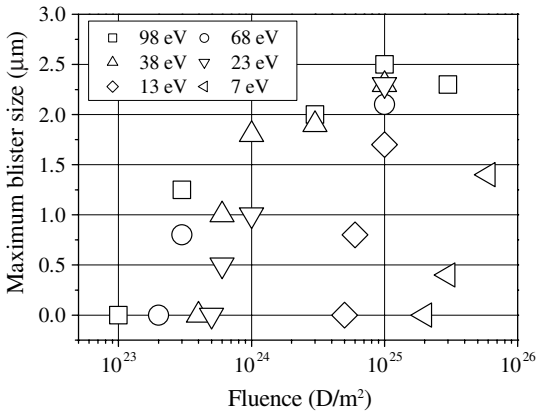

Fig. 2. Maximum blister size as a function of fluence under different incident energies.

hydrogen diffusing deeper will eventually be trapped atomically by such various defects as vacancies, dislocations, impurities, grain boundaries, and internal surface of voids existing intrinsically or being induced during implantation. The hydrogen may also precipitate as gaseous phase within the existing voids and/or new cavities nucleating at the existing defects, driven by high chemical potential due to buildup to high concentration in solution if the implanted hydrogen is not very mobile [14]. The flow of deuterium into voids may lead to gas pressures high enough to cause the void volume to increase by punching out self-interstitial loops [15]. Then the pressure drops and more hydrogen can be accommodated in the voids. This process repeats and the voids grow up and coalesce each other by the inter-bubble fracture mechanism [15]. The cavity coalescence will eventually lead to blistering of the overlying layer.

Deuterium atoms with energies less than 1 keV are not able to produce displacement damage in tungsten [10]. Thus the intrinsic defects, together with surface structure under plasma beam irradiation as to be discussed in the next subsection, play a key role in the present study. For a fixed energy, the fluence tendency observed may be explained as follows. A critical fluence for blistering Φ_{cr} is necessary for accumulation of deuterium into voids so that the pressures inside can be high enough to trigger void growth and coalescence. At the initial stage, blisters appear small in size and rare in number after the Φ_{cr} is reached (most typical for the case of 7 eV/3×10^{25} D/m^2). Then the blisters grow up with further increasing the fluence due mainly to more flow of deuterium into blisters from solution and newly coalesced small neighboring voids. Also new blisters keep emerging and distribute at the surface. The blister growth in the present study seems to saturate at 2–3 μm in diameter from quite small fluences on. For example, as shown in Figs. 1 and 2, in the case of 38 eV, some blisters of ~2 μm have already appeared at the fluence of 1×10^{24} D/m^2. Increase in the fluence to 3×10^{24} and 1×10^{25} D/m^2 does not change the size significantly. This may be attributed to possible rupture of blisters at certain sizes, dependent probably on the cap thicknesses of blisters and the material properties like yield stress and surface tension, as indicated by Evans [15] and Kamada and Higashida [16] in their studies on the radiation blistering by helium implantation. Evidence of rupture in this study was indeed found as shown in Fig. 3 for 38 eV/1×10^{25} D/m^2 irradiation where there exist clearly cracks at the periphery of some blisters.

The energy independence of the maximum blister size as observed in Figs. 1 and 2 may be attributed to the too low energies used in the experiments. The ion ranges are only some nanometers for the energies. However, preliminary SEM observation on the cross-section of a blister prepared by focused ion beam (FIB) milling shows the blister cap thickness of ~0.4 μm and the blister diameter of ~1.7 μm. The cap thickness is about two orders of magnitude larger than the ion ranges. This reflects that the deuterium distribution does not follow the ion range at such low energies, since hydrogen diffuses in most metals at room temperature and above [17]. It is possible that it is the much deeper diffusion that is responsible to the energy independence behavior. Some pairs of images in Fig. 1, e.g., 38 eV and 98 eV at 3×10^{23} D/m^2, 7 eV and 38 eV at 1×10^{25} D/m^2, 7 eV and 98 eV at 3×10^{25} D/m^2, indicate that larger incident energy results in earlier blistering and faster evolution. This may be briefly explained as follows: larger incident energy favors deeper penetration of more implanted deuterium, allowing quicker buildup of pressures and thus earlier blistering and faster evolution. More discussion on energy dependence will be made in the following subsection.

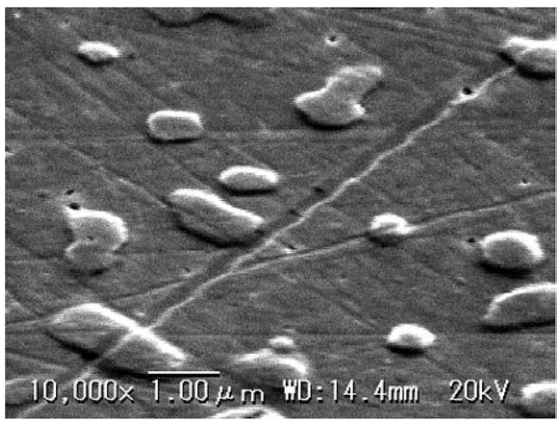

Fig. 3. Surface morphology of the sample of 38 eV/1×10^{25} D/m^2 irradiation showing cracks along the periphery of some blisters.

3.2. Energy dependence of the critical fluence for blistering

Based on the SEM observation, Φ_{cr} under different incident energies can be extracted and shown in Fig. 4. There exists a parameters window above the curve within which blistering occurs. Φ_{cr} increases with decreasing the incident energy, and the curve has a turning point around 20 eV/D, probably implying a change in the underlying mechanisms for the blistering behavior. Under irradiations at such low energies as employed in this work, the surface structure under plasma beam irradiation most likely play a key role. The naturally oxidized layer after polishing was estimated to be stable WO_3 of about 1–2 nm thick [18,19]. XPS analysis has been performed on the surfaces unirradiated and irradiated to different fluences at an incident energy of 38 eV. Spectra for W are shown in Fig. 5, showing two kinds of peaks originated from bulk W (W4f7/2 and W4f5/2) and W oxide (W–O4f7/2 and W–O4f5/2), and absence of carbides on the surface, determined by taking together the corresponding O and C spectra into consideration. Carbon exists probably in the form of adsorbed species on the surfaces in all cases. The analysis suggests the presence of the oxide layers of only several monolayers in all cases, corresponding to the depth resolution of XPS analysis since in all cases, the bulk W peaks appeared. The analysis shows that there is no time-dependent growth/deposition of surface layers as the irradiation time was varied by 17 times for the two fluences, consistent with no obvious impurities in the plasmas [13]. The thicker oxide layers after irradiation might be due to irradiation-induced in situ residual gases incorporation or surface activation-induced ex situ incorporation when exposing in air after irradiation. However, even if the oxide layer got thick due to the former cause, the layer seemed to become stable at a quite small fluence (only irradiation of tens of seconds) and the final thickness was still some monolayers. The surface oxide layer was further analyzed by SIMS depth profiling that provides us with continuous depth information of elemental distribution fully automatically during the sputtering process. The spectra are depicted in Fig. 6, with the Y-axis expressed as a ratio of O and W counts for relative comparison. In the figure, the oxide layers of the samples unirradiated and irradiated were removed after being sputtered for about 50 and 100 s, corresponding to thicknesses of about 0.8 and 1.5 nm, respectively, based on the sputtering rate of ~0.015 nm/s estimated by the surface profiler. The results are quite consistent with what observed in the XPS analysis, i.e., the layers being always within some monolayers thick and the layers after irradiation thicker than unirradiated.

A simple model may be presented as illustrated in Fig. 7 to describe how the surface structure impacts on

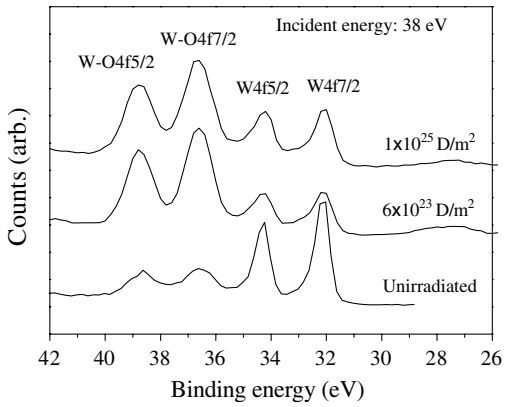

Fig. 5. XPS spectra of the surfaces unirradiated and irradiated to different fluences at an incident energy of 38 eV/D. Meaning of symbols: W4f7/2 and W4f5/2 – bulk W peaks, W–O4f7/2 and W–O4f5/2 – W oxide peaks.

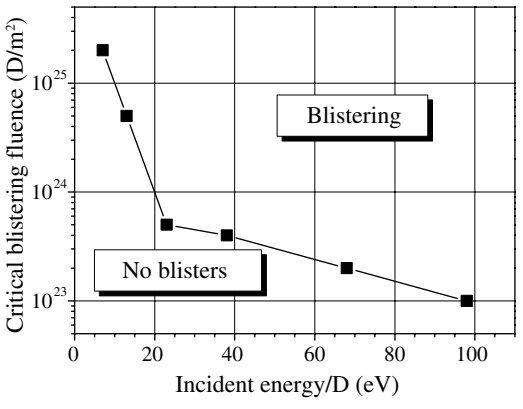

Fig. 4. Critical fluence for blistering as a function of incident energy.

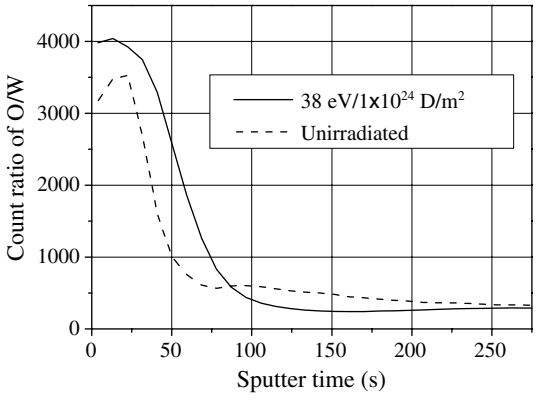

Fig. 6. SIMS spectra showing the surface oxide layers on an unirradiated sample and the sample of 38 eV/1×10^{24} D/m^2 irradiation.

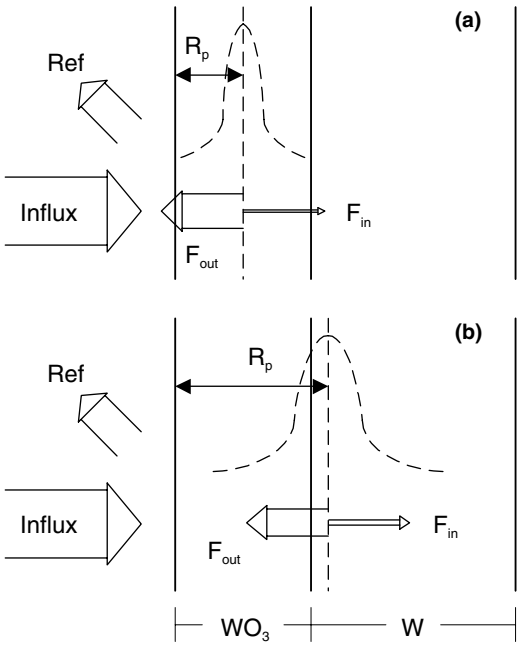

Fig. 7. A surface barrier model for uptake and release of deuterium in W, (a) at very low energies; (b) at penetration energies. Meaning of symbols: Influx – incident flux, Ref – reflection, R_p – ion range, F_{in} – inward moving flux, F_{out} – outward moving flux, and dotted curves – Gaussian distribution of the ion range.

the uptake and release of deuterium into and out of W being irradiated, and in turn on the energy dependence of Φ_{cr}. Reference data in Table 1 for the ion range R_p appeared in Fig. 7 are collected from literature [18] or calculated by computer code like SRIM [20]. In general, more than half of the incident particles are reflected back to vacuum at low incident energies [18]. The implanted deuterium is eventually divided into two parts, a great fraction moving outwards and desorbing from the surface into vacuum and the rest moving inwards and finally being trapped or precipitated in the bulk. At very low energies, the ion ranges are so short that their distributions peak within the oxide layer, as shown in Fig. 7(a). The inward diffusion is hampered by the oxide layer and the interface between the oxide layer and the bulk acting as an uptake barrier as suggested by Richards et al. [21]. Thus only a very small fraction of the implanted deuterium can enter the bulk, leading to obviously much longer time for nucleation of new voids and buildup of pressures in voids in the bulk, and as a result, the Φ_{cr} becomes very large. With increasing the energy, the ion range distribution may peak in the bulk, as depicted in Fig. 7(b), indicating that most of projectiles penetrate through the oxide layer and the diffusion starts from the depth R_p. And now the oxide layer may act as a release barrier, resulting in relatively much more inward diffusion and as a consequence much smaller Φ_{cr}. The transition from (a) to (b) in Fig. 7 may be responsible for the turning point around 20 eV/D in Fig. 4, implying start of the penetration, which roughly matches the calculated ion range and the observed layer thickness. Within the two ranges of the incident energy of 7–20 eV/D and 20–98 eV/D, Φ_{cr} decreases with increasing the energy, due simply to more and faster uptake.

Table 1
Ion ranges R_p (nm) collected from Ref. [18] (D → W) and calculated using SRIM2003 [20] (D → WO_3)

E (eV)	200	100	50	20	10
R_p(D → W)	6.3	4.4	3.0	1.9	1.3
R_p(D → WO_3)	4.8	3.6	2.3	1.3	0.9

One point worthy of discussion herein is a possible sputtering effect of impurities in ion and plasma beams, mainly in the form of oxygen or carbon related species. The impurities, if any, may induce surface erosion significantly even at quite low energies due to their much larger masses than deuterium [18]. A natural extension of our model proposed above predicts that if the incident energy or the fraction of heavier impurities in plasma is large enough to generate significant sputtering on the W surface, especially on WO_3 with a lower surface binding energy, a second turning point for the Φ_{cr} curve in Fig. 2 could be expected when the thin oxide layer is removed quickly, and disappearance of the release barrier raises Φ_{cr} greatly. This did not occur within our experimental range of <100 eV/D, indicating negligible sputtering in our experiments. Ye et al. [11] also argued for negligible sputtering in their plasma irradiation at low energy (<100 eV). However, Hirooka et al. [22] reported that the O atoms in OH^+ and H_2O^+ ions ionized from the H_2O vapor existing in the chamber as main residual gas affected the erosion behavior of tungsten being irradiated by deuterium plasma beams, particularly at energies below 250 eV/D or so within which sputtering by D incidence is negligible [18]. And H_2O vapor was considered to be the main source to generate plasma impurities for electron temperatures ranging from 7 to 30 eV. Therefore the electron temperature is the controlling factor for the formation of these O-related impurities. In our plasma, the electron temperature was measured to be <4 eV, which did not favor the impurity formation in the plasma, and was also consistent with no obvious impurities in the plasmas [13].

4. Conclusions

Polycrystalline samples of 99.99% pure tungsten were exposed at near room temperature to deuterium plasma beams with a fixed high flux of 1×10^{22} D/m^2/s, energies ranging 7–98 eV/D, and fluences up to 6×10^{25} D/m^2.

Conclusions may be drawn from the experiments as follows:

(1) At each incident energy, blisters were observed at the irradiated surface of W samples after a corresponding critical fluence was achieved.
(2) The blisters increased in their size and number with fluence at low fluences. The size increase tended to saturate at certain fluences within the experimental fluence ranges, which might be attributed to rupturing of blisters.
(3) The critical fluence for blistering Φ_{cr} was found to increase with decreasing the incident energy with a turning point at energy around 20 eV/D, due probably to the barrier effect of the oxide layer on W on both deuterium release from and uptake into the bulk W.

Acknowledgements

The authors would like to express their sincere gratitude to Drs M. Seki, S. Seki, H. Takatsu and H. Tsuji (JAERI) for their encouragement and support to this work. Thanks also to Drs H. Nakamura and Y. Ishimoto (JAERI) for their assistance in XPS and SIMS analyses, respectively.

References

[1] ITER Physics Basis, Nucl. Fusion 39 (1999) 2137.
[2] ITER Technical Basis, ITER EDA Documentation Series, No. 24, IAEA, 2002.
[3] V. Philipps, R. Neu, J. Rapp, U. Samm, M. Tokar, T. Tanabe, M. Rubel, Plasma Phys. Control. Fusion 42 (2000) B293.
[4] H. Bolt, V. Barabash, G. Federici, J. Linke, A. Loarte, J. Roth, K. Sato, J. Nucl. Mater. 307–311 (2002) 43.
[5] N. Yoshida, J. Nucl. Mater. 266–269 (1999) 197.
[6] S.M. Myers, P.M. Richards, W.R. Wampler, J. Nucl. Mater. 165 (1989) 9.
[7] Fan C. Sze, Russ P. Doerner, Stan Luckhardt, J. Nucl. Mater. 264 (1999) 89.
[8] T. Venhaus, R. Causey, R. Doerner, T. Abeln, J. Nucl. Mater. 290–293 (2001) 505.
[9] Wenming Wang, J. Roth, S. Lindig, C.H. Wu, J. Nucl. Mater. 299 (2001) 124.
[10] K. Tokunaga, R.P. Doerner, et al., J. Nucl. Mater. 307–311 (2002) 126.
[11] M.Y. Ye, H. Kanehara, S. Fukuta, N. Ohno, S. Takamura, J. Nucl. Mater. 313–316 (2003) 72.
[12] G.-N. Luo, W.M. Shu, H. Nakamura, S. O'hira, T. Hayashi, M. Nishi, JAERI-Tech 031 (2004) 1.
[13] G.-N. Luo, W.M. Shu, H. Nakamura, S. O'hira, M. Nishi, Rev. Sci. Instrum. 75 (11) (2004) 4374.
[14] G. Federici, C.H. Skinner, et al., Nucl. Fusion 41 (12R) (2001) 1967.
[15] J.H. Evans, J. Nucl. Mater. 68 (1977) 129, 76/77 (1978) 228.
[16] K. Kamada, Y. Higashida, J. Appl. Phys. 50 (6) (1979) 4131.
[17] H. Wipf, Diffusion of Hydrogen in Metals, Springer Topics in Applied Physics, vol. 73, Springer-Verlag, Berlin, 1997.
[18] W. Eckstein, IPP-Report 9/132, 2002, p. 1.
[19] D.P. Jackson, W. Eckstein, Nucl. Instrum. Methods 194 (1982) 671.
[20] http://www.srim.org/.
[21] P.M. Richards, S.M. Myers, W.R. Wampler, D.M. Follstaedt, J. Appl. Phys. 65 (1) (1989) 180.
[22] Y. Hirooka, M. Bourham, et al., J. Nucl. Mater. 196–198 (1992) 149.